Research Article Vol. 57, No. 27 / 20 September 2018 / Applied Optics 7857

applied optics

Self-correction of alignment errors and retardations for a channeled spectropolarimeter

Wenhe Xing,[1,2] Xueping Ju,[1,2] Changxiang Yan,[1,*] Bin Yang,[3] and Junqiang Zhang[1,3]

[1]Changchun Institute of Optics, Fine Mechanics and Physics, Chinese Academy of Sciences, Changchun 130033, China
[2]University of Chinese Academy of Sciences, Beijing 100049, China
[3]Yusense Information Technology and Equipment (Qingdao) Inc., Qingdao 266000, China
*Corresponding author: yancx0128@126.com

Received 2 July 2018; revised 22 August 2018; accepted 22 August 2018; posted 22 August 2018 (Doc. ID 336558); published 13 September 2018

Alignment errors of birefringent retarders and retardation errors introduced by environmental perturbations can cause significant influences on reconstructed Stokes parameters for the channeled spectropolarimeter. In this paper, we propose what we believe is a novel self-correction model that is independent of input polarization parameters to reduce the effects of alignment errors and environmental perturbations. This self-correction method can realize calibration and compensation of alignment errors and retardations simultaneously by measuring the target light in orbit. Simulation results show that alignment errors and retardations can be calibrated accurately, and the reconstructed Stokes parameters by using the presented method are more precise than by using the traditional method. The validity and feasibility of the presented method are further confirmed through experiments in the presence of alignment errors and environmental perturbations.

https://doi.org/10.1364/AO.57.007857

1. INTRODUCTION

In the past several decades, spectropolarimetry has rapidly developed due to its ability of acquiring the spectral content and the polarization state of light. It is of particular importance for several applications, including atmospheric aerosol characterization [1,2], remote sensing [3–7], and material characterization [8–12]. Two different classical modulation principles are discerned: spatial and temporal modulation. In the case of spatial modulation, the division into several beams significantly increases an instrument's size and mechanical complexity. With temporal modulation, moving parts are undesirable from the standpoint of reliability. It also limits ability to acquire data on rapidly changing scenes, such as moving targets or targets viewed from moving platforms [13].

In 1999, Oka and Iannarilli first described the channeled spectropolarimetry, an attractive approach for polarimetry [14,15], by which we can eliminate the disadvantages of conventional modulation principles. This technique can offer a direct measurement of spectrum and the polarization state of the light, as compared with an indirect (multiplexed) measurement by spatial modulation. Based on a snapshot mode, this technique can reduce the temporal registration error compared with the temporal modulation [5]. With a simple optical system and no movable polarization components, the entire wavelength-dependent state of polarization (SOP) and spectral information of a scene can be acquired simultaneously. The channeled spectropolarimetry has been widely used in polarimetry.

Despite these benefits, there are still many vital problems with polarimetric spectral intensity modulation (PSIM) when the channeled spectropolarimeter is applied in orbit. Specifically, alignment errors of the retarders, which have significant influences on the reconstructed Stokes parameters, are inevitable for the manufacturing and alignment tolerances. Furthermore, retardations, another key factor for reconstructed Stokes parameters, are quite susceptible to environmental perturbations, such as temperature variation [16] and stress [17].

Mu *et al.* [18], Yang *et al.* [19] and Ju *et al.* [20] have calibrated and compensated alignment errors by reference beam or additional components. However, they have not considered the effects of environmental conditions. Their methods are more suitable for calibration in the laboratory. By using their methods, the stability of the instrument applied in orbit cannot be guaranteed. Taniguchi and Oka [21] have proposed a self-calibration method that can reduce the effects of temperature change. However, they have not considered the alignment errors of retarders, which are inevitable. On the one hand, with the inevitable alignment errors, this self-calibration method would reduce the measurement accuracy. On the other hand, this method would lose efficacy even after the accurate calibration of alignment errors in the laboratory.

Locke *et al.* [22] used a 3:1 ratio of retarder thickness to check the system alignments. Compared with a 1:2 ratio, the 3:1 ratio introduces two channels into the Fourier domain, and the two channels contain the alignment errors information

in the system, but the principles of operation of the system are otherwise unchanged [23]. However, this method can only realize qualitative measurement. In this paper, a novel method is proposed to calibrate and compensate alignment errors and retardations of the retarders simultaneously. With a 3:1 ratio of retarder thickness considering alignment errors in the system, we derive a new model to reconstruct Stokes parameters by target light. In this model, alignment errors and retardations are unknown quantities. Then, we eliminate the phase terms and input polarization parameters by the operations among channels to self-calibrate the alignment errors. After that, we can calculate phase terms based on the calibrated alignment errors and the information of channels. Thus, we realize the self-correction of alignment errors and retardations to reduce the effects of alignment errors and environmental perturbations by target light.

This paper is organized as follows: Section 2 provides an overview of the principle of the channeled spectropolarimetry. Section 3 derives a theoretical model of self-correction. In Sections 4 and 5, we analyze and summarize our simulation and experimental results, respectively. The conclusion is presented in Section 6.

2. PRINCIPLE OF CHANNELED SPECTROPOLARIMETRY

We first briefly review the principle of channeled spectropolarimetry. The schematic diagram of a channeled spectropolarimeter in ideal condition is illustrated in Fig. 1. A polychromatic beam $S(\sigma)$ passes through two retarders, R_1 and R_2, with thicknesses d_1 and d_2, respectively, and a linear analyzer, A, and then the exiting light is recorded by a spectrometer. The fast axis of R_1 is aligned with the transmission axis of A, and R_2 is oriented with its fast axis at 45° to the transmission axis of A in an ideal condition.

A. Classical Model of Reconstructed Stokes Parameters

If the incident Stokes vector is $S_{\text{in}} = [S_0, S_1, S_2, S_3]^T$ (where T denotes the transpose operation), the Stokes vector of the target light passing through the system can be given by [14]

$$S_{\text{out}}(\sigma) = M_A(0°) \cdot M_{R_2}[45°, \varphi_2(\sigma)] \cdot M_{R_1}[0°, \varphi_1(\sigma)] \cdot S_{\text{in}}(\sigma), \tag{1}$$

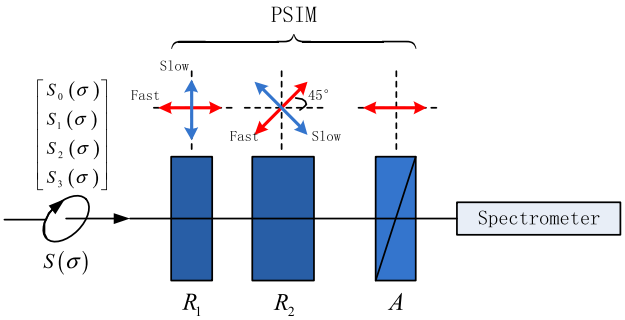

Fig. 1. Schematic of the channeled spectropolarimeter in an ideal condition.

where M_A, M_{R_2}, and M_{R_1} denote the Mueller matrices of A, R_2, and R_1, respectively, and $\varphi_2(\sigma)$ and $\varphi_1(\sigma)$ are the ideal phase retardations of R_2 and R_1, respectively. The spectrum obtained by the spectrometer can be described as

$$\begin{aligned} B(\sigma) = {} & \frac{1}{2}S_0(\sigma) + \frac{1}{4}S_1(\sigma)\{\exp[-i\varphi_2(\sigma)] + \exp[i\varphi_2(\sigma)]\} \\ & + \frac{1}{8}S_{23}(\sigma)\exp\{-i[\varphi_1(\sigma) - \varphi_2(\sigma)]\} \\ & + \frac{1}{8}S_{23}^*(\sigma)\exp\{i[\varphi_1(\sigma) - \varphi_2(\sigma)]\} \\ & - \frac{1}{8}S_{23}(\sigma)\exp\{-i[\varphi_1(\sigma) + \varphi_2(\sigma)]\} \\ & - \frac{1}{8}S_{23}^*(\sigma)\exp\{i[\varphi_1(\sigma) + \varphi_2(\sigma)]\}, \end{aligned} \tag{2}$$

where $S_{23}(\sigma) = S_2(\sigma) + iS_3(\sigma)$, and $\varphi_j(\sigma) = 2\pi L_j\sigma = 2\pi\Delta n(\sigma)d_j\sigma = \varphi_{0j}(\sigma) + 2n_j(\sigma)\pi$, $(j = 1, 2)$, $L_j = \Delta n(\sigma)d_j$ is the optical path difference (OPD) introduced by R_j, $\Delta n(\sigma)$ is the birefringence of the birefringent crystal, $\varphi_{0j}(\sigma)$ is the zero order retardation and $n_j(\sigma)$ is dependent on the thickness of the retarder. Based on Eq. (2), the seven phase terms represent seven distinct channels in the Fourier domain that contain the data related to the input polarization parameters S_0, S_1, S_2, and S_3. Calculating the autocorrelation of $B(\sigma)$ using the Fourier transformation, we can distribute the seven channels with seven phase terms:

$$\begin{aligned} C(L) = {} & C_0(L) + C_1(L - L_2) + C_{-1}(-L - L_2) \\ & + C_2[L - (L_1 - L_2)] + C_{-2}[-L - (L_1 - L_2)] \\ & + C_4[L - (L_1 + L_2)] + C_{-4}[-L - (L_1 + L_2)], \end{aligned} \tag{3}$$

where

$$C_0 = \mathcal{F}\left\{\frac{1}{2}S_0(\sigma)\right\}, \tag{4a}$$

$$C_1 = \mathcal{F}\left\{\frac{1}{4}S_1(\sigma)\exp[-i\varphi_2(\sigma)]\right\}, \tag{4b}$$

$$C_{-1} = \mathcal{F}\left\{\frac{1}{4}S_1(\sigma)\exp[i\varphi_2(\sigma)]\right\}, \tag{4c}$$

$$C_2 = \mathcal{F}\left\{\frac{1}{8}S_{23}(\sigma)\exp\{-i[\varphi_1(\sigma) - \varphi_2(\sigma)]\}\right\}, \tag{4d}$$

$$C_{-2} = \mathcal{F}\left\{\frac{1}{8}S_{23}^*(\sigma)\exp\{i[\varphi_1(\sigma) - \varphi_2(\sigma)]\}\right\}, \tag{4e}$$

$$C_4 = \mathcal{F}\left\{-\frac{1}{8}S_{23}(\sigma)\exp\{-i[\varphi_1(\sigma) + \varphi_2(\sigma)]\}\right\}, \tag{4f}$$

$$C_{-4} = \mathcal{F}\left\{-\frac{1}{8}S_{23}^*(\sigma)\exp\{i[\varphi_1(\sigma) + \varphi_2(\sigma)]\}\right\}, \tag{4g}$$

and L denote the frequency variable that is conjugate to wavenumber σ under the Fourier transform [24]. The seven channels center at $L = 0$, $\pm L_2$, $\pm(L_1 - L_2)$, and $\pm(L_1 + L_2)$, respectively. Then by filtering out seven channels and performing inverse Fourier transformations independently, the whole Stokes parameters of the target light can be described as

$$S_0(\sigma) = 2\mathcal{F}^{-1}\{C_0\}, \tag{5a}$$

$$S_1(\sigma) = \frac{4 \times \mathcal{F}^{-1}\{C_1\}}{\exp[-i\varphi_2(\sigma)]}, \tag{5b}$$

$$S_2(\sigma) = -\mathrm{Re}\left\{\frac{8 \times \mathcal{F}^{-1}\{C_4\}}{\exp\{-i[\varphi_1(\sigma) + \varphi_2(\sigma)]\}}\right\}, \tag{5c}$$

$$S_3(\sigma) = -\mathrm{Im}\left\{\frac{8 \times \mathcal{F}^{-1}\{C_4\}}{\exp\{-i[\varphi_1(\sigma) + \varphi_2(\sigma)]\}}\right\}, \tag{5d}$$

where Re is the operator to extract the real part, and Im is the operator to extract the imaginary part.

B. Current Reference Beam Calibration Technique

In Eqs. (5a)–(5d), $\exp[-i\varphi_2(\sigma)]$ and $\exp\{-i[\varphi_1(\sigma) + \varphi_2(\sigma)]\}$ are undetermined. In the traditional method, a reference beam linearly polarized oriented at 22.5° [18,25] is used to determine the phase terms. The Stokes parameters of the 22.5° linearly polarized reference beam are given by

$$S_1(\sigma) = \sqrt{2}/2 S_0(\sigma), \tag{6a}$$

$$S_2(\sigma) = \sqrt{2}/2 S_0(\sigma), \tag{6b}$$

$$S_3(\sigma) = 0. \tag{6c}$$

Combining Eqs. (4a)–(4g) and Eqs. (6a)–(6c), we can obtain the phase terms, i.e.,

$$\exp[-i\varphi_2(\sigma)] = 2\sqrt{2}\frac{\mathcal{F}^{-1}\{C_{1,22.5°}\}}{\mathcal{F}^{-1}\{C_{0,22.5°}\}}, \tag{7a}$$

$$\exp\{-i[\varphi_1(\sigma) + \varphi_2(\sigma)]\} = -4\sqrt{2}\frac{\mathcal{F}^{-1}\{C_{4,22.5°}\}}{\mathcal{F}^{-1}\{C_{0,22.5°}\}}. \tag{7b}$$

Lastly, substituting the calibrated phase terms, $\exp[-i\varphi_2(\sigma)]$ and $\exp\{-i[\varphi_1(\sigma) + \varphi_2(\sigma)]\}$, into Eqs. (5a)–(5d), the whole Stokes parameters of the target light can be obtained. However, this reconstruction procedure is suitable only for the spectropolarimeter in an ideal condition. When working with alignment errors and environmental perturbations, the accuracy of the reconstructed Stokes parameters and the stability of the instrument will be reduced by using this reconstruction model.

3. SELF-CORRECTION MODEL OF RECONSTRUCTED STOKES PARAMETERS

In this section, a novel method is proposed to calibrate and compensate alignment errors and retardations of the retarders simultaneously. A two-setup approach is adopted for the self-correction method. We first derive a new model of reconstructed Stokes parameters, and then determine the unknown quantities, alignment errors, and retardations in the new model by self-calibration.

A. Derivation of the Self-Correction Model

When the system is working in an actual condition, the angle errors, ε_1 and ε_2, of R_1 and R_2, respectively, are inevitable, as shown in Fig. 2. The Stokes vector of the target light passing through the system will be expressed as

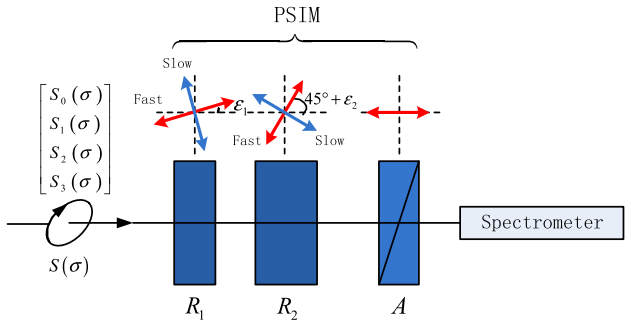

Fig. 2. Schematic of the channeled spectropolarimeter in an actual condition.

$$S'_{\mathrm{out}}(\sigma) = M_A(0°) \cdot M_{R_2}[45° + \varepsilon_2, \varphi_2(\sigma)] \cdot M_{R_1}[\varepsilon_1, \varphi_1(\sigma)] \cdot S_{\mathrm{in}}(\sigma). \tag{8}$$

And the spectrum obtained by the spectrometer will be described as

$$\begin{aligned} B'(\sigma) = {} & \frac{1}{2}[S_0(\sigma) + b_1c_1S_{12}(\sigma)] \\ & + \frac{1}{4}b_2c_2S_{12}(\sigma)\{\exp[-i\varphi_2(\sigma)] + \exp[i\varphi_2(\sigma)]\} \\ & - \frac{1}{8}b_2(1 + c_1)S^*_{123}(\sigma)\exp\{-i[\varphi_1(\sigma) - \varphi_2(\sigma)]\} \\ & - \frac{1}{8}b_2(1 + c_1)S_{123}(\sigma)\exp\{i[\varphi_1(\sigma) - \varphi_2(\sigma)]\} \\ & + \frac{1}{4}b_1c_2S^*_{123}(\sigma)\exp[-i\varphi_1(\sigma)] \\ & + \frac{1}{4}b_1c_2S_{123}(\sigma)\exp[i\varphi_1(\sigma)] \\ & + \frac{1}{8}b_2(1 - c_1)S^*_{123}(\sigma)\exp\{-i[\varphi_1(\sigma) + \varphi_2(\sigma)]\} \\ & + \frac{1}{8}b_2(1 - c_1)S_{123}(\sigma)\exp\{i[\varphi_1(\sigma) + \varphi_2(\sigma)]\}, \end{aligned} \tag{9}$$

where

$$\begin{cases} a_1 = \sin 2\varepsilon_1 \\ a_2 = \cos 2\varepsilon_1 \end{cases}, \quad \begin{cases} b_1 = \sin 2\varepsilon_2 \\ b_2 = \cos 2\varepsilon_2 \end{cases}, \quad \begin{cases} c_1 = \sin 2(\varepsilon_2 - \varepsilon_1) \\ c_2 = \cos 2(\varepsilon_2 - \varepsilon_1) \end{cases}, \tag{10}$$

$$\begin{cases} S_{12}(\sigma) = a_2S_1(\sigma) + a_1S_2(\sigma) \\ S_{123}(\sigma) = a_1S_1(\sigma) - a_2S_2(\sigma) + iS_3(\sigma) \end{cases}. \tag{11}$$

Based on Eq. (9), there are nine distinct channels in the Fourier domain; the Fourier transformation of $B'(\sigma)$ is given by

$$\begin{aligned} C'(L) = {} & C'_0(L) + C'_1(L - L_2) + C'_{-1}(-L - L_2) \\ & + C'_2[L - (L_1 - L_2)] + C'_{-2}[-L - (L_1 - L_2)] \\ & + C'_3(L - L_1) + C'_{-3}(-L - L_1) \\ & + C'_4[L - (L_1 + L_2)] + C'_{-4}[-L - (L_1 + L_2)], \end{aligned} \tag{12}$$

where

$$C_0' = \mathcal{F}\left\{\frac{1}{2}[S_0(\sigma) + b_1c_1S_{12}(\sigma)]\right\}, \tag{13a}$$

$$C_1' = \mathcal{F}\left\{\frac{1}{4}b_2c_2S_{12}(\sigma)\exp[-i\varphi_2(\sigma)]\right\}, \tag{13b}$$

$$C_{-1}' = \mathcal{F}\left\{\frac{1}{4}b_2c_2S_{12}(\sigma)\exp[i\varphi_2(\sigma)]\right\}, \tag{13c}$$

$$C_2' = \mathcal{F}\left\{-\frac{1}{8}b_2(1+c_1)S_{123}^*(\sigma)\exp\{-i[\varphi_1(\sigma)-\varphi_2(\sigma)]\}\right\}, \tag{13d}$$

$$C_{-2}' = \mathcal{F}\left\{-\frac{1}{8}b_2(1+c_1)S_{123}(\sigma)\exp\{i[\varphi_1(\sigma)-\varphi_2(\sigma)]\}\right\}, \tag{13e}$$

$$C_3' = \mathcal{F}\left\{\frac{1}{4}b_1c_2S_{123}^*(\sigma)\exp[-i\varphi_1(\sigma)]\right\}, \tag{13f}$$

$$C_{-3}' = \mathcal{F}\left\{\frac{1}{4}b_1c_2S_{123}(\sigma)\exp[i\varphi_1(\sigma)]\right\}, \tag{13g}$$

$$C_4' = \mathcal{F}\left\{\frac{1}{8}b_2(1-c_1)S_{123}^*(\sigma)\exp\{-i[\varphi_1(\sigma)+\varphi_2(\sigma)]\}\right\}, \tag{13h}$$

$$C_{-4}' = \mathcal{F}\left\{\frac{1}{8}b_2(1-c_1)S_{123}(\sigma)\exp\{i[\varphi_1(\sigma)+\varphi_2(\sigma)]\}\right\}. \tag{13i}$$

The nine channels center at $L = 0$, $\pm L_2$, $\pm(L_1 - L_2)$, $\pm L_1$, and $\pm(L_1 + L_2)$, respectively. However, when the thickness ratio of two retarders is 1:2, channels C_2' and C_{-3}', C_{-2}', and C_3' will be overlapped, respectively. The information in these channels cannot be employed. In this paper, we use a 3:1 ratio to separate the nine channels from one another in the Fourier domain and utilize the information of nine channels completely to realize self-correction. Figure 3 shows the magnitude of the autocorrelation function of the modulated spectrum with the 3:1 ratio. $I\{C_3\} = I\{C_{-3}\} \neq 0$ when the retarders have alignment errors, so that we can find out more information.

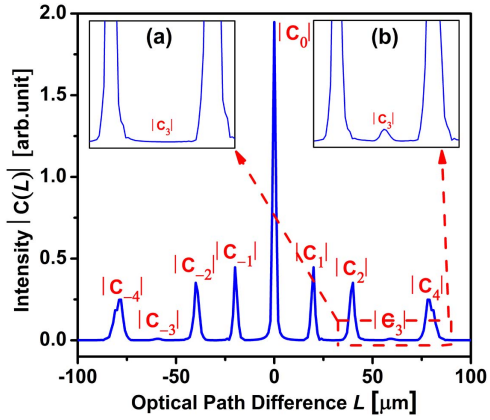

Fig. 3. Magnitude of the autocorrelation function of the modulated spectrum. The enlarged part in the dashed box shows $|C_3|$ (a) without alignment errors and (b) with alignment errors.

By filtering out nine channels and performing inverse Fourier transformations independently, the whole Stokes parameters of the target light can be described as

$$S_0(\sigma) = 2\mathcal{F}^{-1}\{C_0'\} - b_1c_1E_1, \tag{14a}$$

$$S_1(\sigma) = a_2E_1 + a_1\mathrm{Re}\{E_2\}, \tag{14b}$$

$$S_2(\sigma) = a_1E_1 - a_2\mathrm{Re}\{E_2\}, \tag{14c}$$

$$S_3(\sigma) = -\mathrm{Im}\{E_2\}, \tag{14d}$$

where

$$\begin{cases} E_1 = \dfrac{4\times\mathcal{F}^{-1}\{C_1'\}}{b_2c_2\times\exp[-i\varphi_2(\sigma)]} \\ E_2 = \dfrac{8\times\mathcal{F}^{-1}\{C_4'\}}{b_2(1-c_1)\times\exp\{-i[\varphi_1(\sigma)+\varphi_2(\sigma)]\}}. \end{cases} \tag{15}$$

B. Self-Calibration of Alignment Errors and Retardations

The demodulation of the Stokes parameters can be performed as long as the alignment errors and retardations can be calibrated precisely. We assume that $\varepsilon_2 > 0$ and $\varepsilon_1 < 0$, which are dependent on the manufacturing and alignment tolerances of the channeled spectropolarimeter. The positive sign of alignment errors indicates that the fast axes of the retarder deviate from their ideal state in a counterclockwise direction, while the negative sign indicates a clockwise direction. To avoid the inconvenience that any term of any channels may be zero, the target beam should meet the condition of $S_1 \neq 0$ or $S_2 \neq 0$ or $S_3 \neq 0$, regardless of the SOP of the beam [19].

With Eqs. (13a)–(13i), we eliminate the input polarization parameters in channels to calculate angle errors and phase retardations, i.e.,

$$\frac{\mathcal{F}^{-1}(C_2')\mathcal{F}^{-1}(C_{-2}')}{\mathcal{F}^{-1}(C_4')\mathcal{F}^{-1}(C_{-4}')} = \left(\frac{1+c_1}{1-c_1}\right)^2, \tag{16}$$

$$\frac{\mathcal{F}^{-1}(C_3')\mathcal{F}^{-1}(C_3')}{\mathcal{F}^{-1}(C_4')\mathcal{F}^{-1}(C_2')} = -4\left(\frac{b_1}{b_2}\right)^2, \tag{17}$$

$$\frac{\mathcal{F}^{-1}(C_3')}{\mathcal{F}^{-1}(C_4')} = \frac{2b_1c_2}{b_2(1-c_1)}\exp[i\varphi_2(\sigma)]. \tag{18}$$

With Eqs. (16)–(18) and the following equations: $a_1^2 + a_2^2 = 1$, $b_1^2 + b_2^2 = 1$, and $c_1^2 + c_2^2 = 1$, the alignment errors and phase factor $\exp[i\varphi_2(\sigma)]$ are obtained as

$$c_1 = \frac{\sqrt{\frac{\mathcal{F}^{-1}(C_2')\mathcal{F}^{-1}(C_{-2}')}{\mathcal{F}^{-1}(C_4')\mathcal{F}^{-1}(C_{-4}')}} - 1}{\sqrt{\frac{\mathcal{F}^{-1}(C_2')\mathcal{F}^{-1}(C_{-2}')}{\mathcal{F}^{-1}(C_4')\mathcal{F}^{-1}(C_{-4}')}} + 1}, \tag{19}$$

$$\frac{b_1}{b_2} = \frac{1}{2}\sqrt{\mathrm{abs}\left(\frac{\mathcal{F}^{-1}(C_3')\mathcal{F}^{-1}(C_3')}{\mathcal{F}^{-1}(C_4')\mathcal{F}^{-1}(C_2')}\right)}, \tag{20}$$

$$\exp[i\varphi_2(\sigma)] = \frac{b_2(1-c_1)}{2b_1c_2}\frac{\mathcal{F}^{-1}(C_3')}{\mathcal{F}^{-1}(C_4')}, \tag{21}$$

where abs stands for the operation of taking the absolute value. Then, the angle errors, ε_1 and ε_2, and the target retardation $\varphi_2(\sigma)$ are given by

$$\varepsilon_1 = \left(\frac{1}{2}\right)\arcsin(c_1) + \left(\frac{1}{2}\right)\arctan\left(\frac{b_1}{b_2}\right), \tag{22}$$

$$\varepsilon_2 = \left(\frac{1}{2}\right)\arctan\left(\frac{b_1}{b_2}\right), \tag{23}$$

$$\begin{aligned}[\varphi_2(\sigma)]_{\text{target}} &= \varphi_{02}(\sigma) + 2n_2(\sigma)\pi \\ &= \arg\left[\frac{b_2(1-c_1)}{2b_1c_2}\frac{\mathcal{F}^{-1}(C_3')}{\mathcal{F}^{-1}(C_4')}\right] + 2n_2(\sigma)\pi.\end{aligned} \tag{24}$$

To calibrate the phase factors, we just need to measure $\exp[-i\varphi_2(\sigma)]$ and $\exp\{-i[\varphi_1(\sigma)+\varphi_2(\sigma)]\}$ by referring to the conventional reference beam calibration technique described in Subsection 2.B. While $\exp[-i\varphi_2(\sigma)]$ has been given by Eq. (21) through Eqs. (13a)–(13i), $\exp\{-i[\varphi_1(\sigma)+\varphi_2(\sigma)]\}$ cannot be acquired directly. Therefore, we use the target retardation $\varphi_2(\sigma)$ acquired by Eq. (24) to calculate the target retardation $\varphi_1(\sigma)+\varphi_2(\sigma)$, shown as Eq. (25), provided that both retarders undergo the same environmental perturbations:

$$[\varphi_1(\sigma)+\varphi_2(\sigma)]_{\text{target}} = \frac{\varphi_{2,22.5}(\sigma)}{[\varphi_1(\sigma)+\varphi_2(\sigma)]_{22.5}}[\varphi_2(\sigma)]_{\text{target}}, \tag{25}$$

where $\varphi_{2,22.5}(\sigma)$ and $[\varphi_1(\sigma)+\varphi_2(\sigma)]_{22.5}$ are the retardations of retarders acquired by a 22.5° linearly polarized reference beam in the laboratory.

Lastly, substituting the self-calibration alignment errors, ε_1 and ε_2, and the self-calibration phase terms, $\exp[-i\varphi_2(\sigma)]$ and $\exp\{-i[\varphi_1(\sigma)+\varphi_2(\sigma)]\}$, into Eqs. (14a)–(14d), the whole Stokes parameters S_0, S_1, S_2, and S_3 of target light could be determined accurately. So far, the model of self-correction of alignment errors and retardations in the channeled spectropolarimeter has been built. Based on the presented method, the reconstructed polarization parameters will be more accurate.

4. SIMULATION ANALYSIS

Simulations will be performed to verify the feasibility and advantages of the presented method. In the simulation, we employ a 30° linearly polarized beam as the target light, and the wavenumber range is 11,916 cm^{-1}–16,282 cm^{-1}. R_1 and R_2 are made of quartz, whose birefringence in the selected wave band can be referred to Ref. [26]; their thicknesses are 6 and 2 mm, respectively. The alignment errors of R_1 and R_2 are $\varepsilon_1 = -0.5°$, and $\varepsilon_2 = 0.5°$, respectively. We compare the phase retardations calibration results and reconstructed polarization parameters with two methods, i.e., a traditional method referring to Section 2, and the new method presented in this paper, referring to Section 3.

We first calibrate the alignment errors of the retarders, as shown in Fig. 4. Table 1 shows the averages and errors of the calculated results of ε_1 and ε_2. Because the angle errors are independent of wavenumber, we can use the averages of the calculated values in different wavenumbers as the final determination results. These results indicate that the alignment errors can be determined accurately by using the presented method, which is the foundation of calculating phase retardations and reconstructing Stokes parameters.

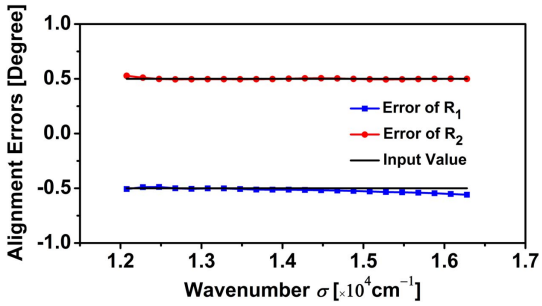

Fig. 4. Calculated results of the alignment errors of R_1 and R_2.

Table 1. Averages and Errors of the Calculated Results of ε_1 and ε_2

Parameter	Input Value	Calculated Value	Error
ε_1	−0.5°	−0.5175°	0.0175°
ε_2	0.5°	0.5006°	0.0006°

Figure 5 shows the calibration results of $\varphi_2(\sigma)$ and $\varphi_1(\sigma)+\varphi_2(\sigma)$. The calibration results obtained by using the presented method almost overlap with the traditional method and the theoretical value of phase retardations. These results indicate that the retardations can be calibrated through the target light in the presented method, which can reduce the effects of environmental perturbations on retardations and improve the stability of the instrument. Figure 6 gives the reconstructed Stokes parameters obtained with the two methods. With the traditional method, which neglects the alignment errors of retarders, the residual errors of normalized Stokes parameters, S_1/S_0, S_2/S_0, and S_3/S_0, over the working wave band are 5.95×10^{-3}, 4.38×10^{-3}, and 5.98×10^{-4}. By using the presented method, the residual errors of S_1/S_0, S_2/S_0, and S_3/S_0 are 4.89×10^{-4}, 9.55×10^{-5}, and 3.23×10^{-4}, respectively; we have reduced the residual errors by 1 or 2 orders of magnitude over the traditional method. The above results indicate that the alignment errors of the retarders have been compensated effectively.

We have provided a simulation of $|\varepsilon_j| = 0.5°$. After that, Monte Carlo simulations will be utilized to prove the general applicability of the presented method with different alignment errors. The amplitude ranges of the alignment errors are 0.3°, 0.4°,…, 1.0° because of the inevitable alignment errors in practical application. During the simulation process, 1000 groups of angle errors, 1000 angle errors of R_1, and 1000 angle errors of R_2 are generated randomly and distributed uniformly in each specific range. Besides, we use the errors of degree of polarization (DOP) [27], given by $\text{DOP}(\sigma) = \sqrt{S_1^2(\sigma)+S_2^2(\sigma)+S_3^2(\sigma)}/S_0(\sigma)$, to analyze the reconstruction results, which are shown in Fig. 7. The errors of DOP are reduced effectively by using the presented method.

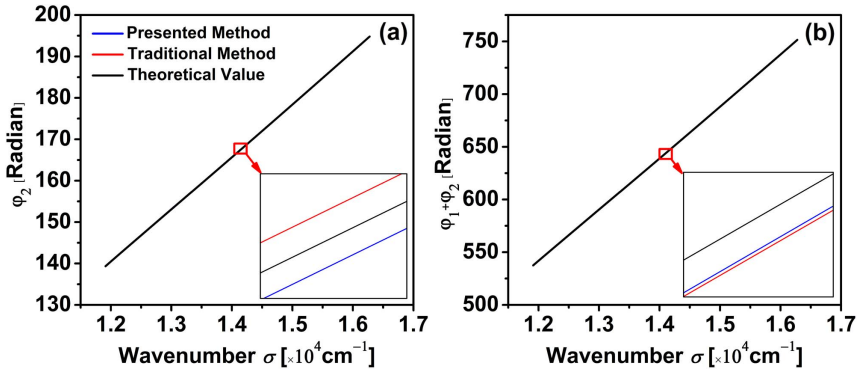

Fig. 5. Calculated results of phase retardations (a) $\varphi_2(\sigma)$ and (b) $\varphi_1(\sigma) + \varphi_2(\sigma)$.

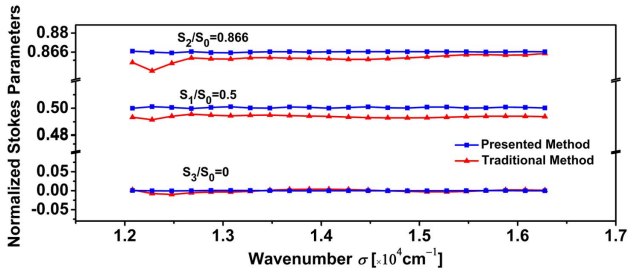

Fig. 6. Reconstructed results of normalized Stokes parameters; theoretical values are $S_1/S_0 = 0.5$, $S_2/S_0 = 0.866$, and $S_3/S_0 = 0$.

And the results tend to definite values with the different angle errors of R_1 and R_2. The Monte Carlo simulations have verified the general applicability of the presented method with different alignment errors.

The simulation results suggest that the angle errors of R_1 and R_2 and the phase terms $\varphi_2(\sigma)$ and $\varphi_1(\sigma) + \varphi_2(\sigma)$ can be calibrated accurately and compensated effectively by using the presented method. The reconstruction Stokes parameters can obtain the same precision with the different angle errors of R_1 and R_2, which means that we can loosen the manufacturing and alignment tolerances of retarders in the channeled spectropolarimeter. The detection results were acquired in the process of each measurement so that the effects of environmental perturbations would be reduced by target light.

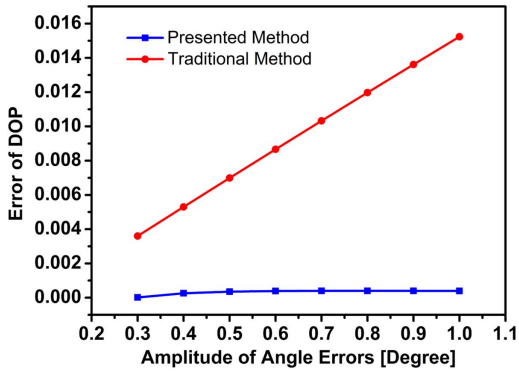

Fig. 7. Error of DOP measurement in the presence of different angle errors.

5. EXPERIMENTAL RESULTS

We carried out an experiment, whose configuration is illustrated in Fig. 8, to further demonstrate the validity of our method. A stabilized tungsten halogen lamp, a collimator, and a rotatable polarizer, P, are used to generate the target beams. The channeled spectropolarimeter consists of the PSIM module and a spectrometer (FieldSpec 3, Analytical Spectral Devices). The thicknesses of R_1, R_2, and the wavenumber range are consistent with the simulation settings.

In order to verify the ability of the present method for compensating alignment and retardation errors, we change the angle error of R_1, ε_1, from −1.5° to −0.5°, and the angle error of R_2, ε_2, from 1.5° to 0.5° with the temperature rising from 24°C to 29°C. The phase retardations may be changed by temperature variation, stress, or other environmental factors in an application. We introduce the temperature variation in this experiment.

Figure 9 gives the reconstructed Stokes parameters under different alignment errors and temperatures with the two methods. The normalized Stokes parameters show significant deviations with the true value by using the traditional method, as shown in Fig. 9(a), and the residual errors of S_1/S_0, S_2/S_0, and S_3/S_0 are 3.62×10^{-2}, 1.34×10^{-1}, and 3.72×10^{-1},

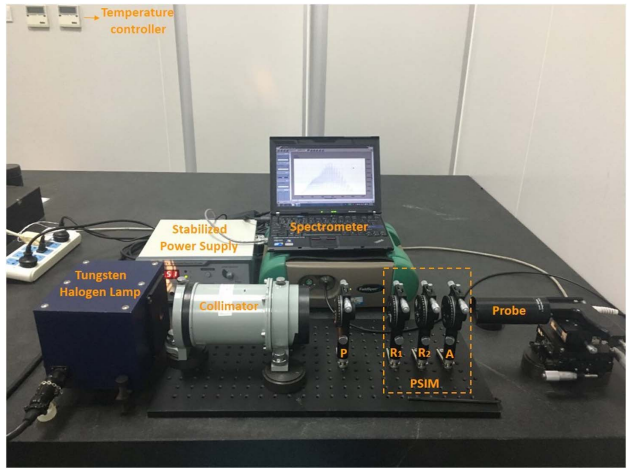

Fig. 8. Experimental setup with a temperature controller to simulate temperature variation in application.

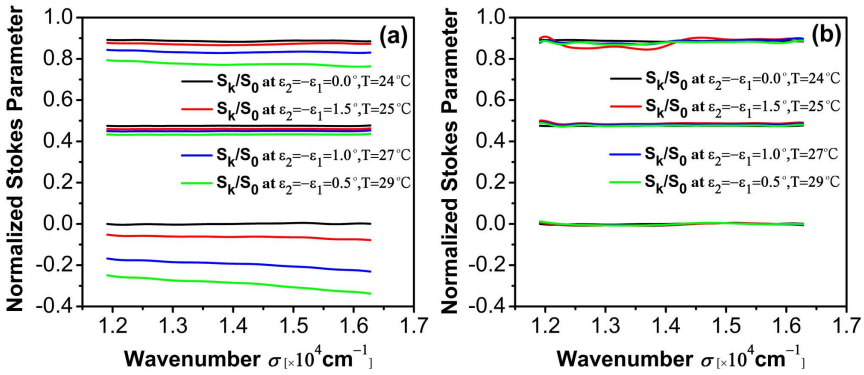

Fig. 9. Reconstructed Stokes parameters from experimental measurements under different alignment errors and temperatures using (a) the traditional method and (b) the presented method. Theoretical reference values are $S_1/S_0 = 0.5$, $S_2/S_0 = 0.866$, and $S_3/S_0 = 0$.

respectively. It is noteworthy that the normalized Stokes parameters under different alignment errors and temperatures almost overlap with each other by using the present method, as shown in Fig. 9(b). The residual errors of S_1/S_0, S_2/S_0, and S_3/S_0 are less than 8.41×10^{-3}, 1.33×10^{-2}, and 8.51×10^{-3}, respectively. Because of the thickness errors of the retarders, noise, and stray light, the experimental reconstruction errors are larger than the simulation results.

The experimental results indicate that by using the self-correction method, the reconstructed Stokes parameters can be acquired accurately even in the presence of different alignment errors and environmental perturbations. The results show good agreement with the simulated analysis over the measured spectral range. This method plays an important role for the in-orbit application of the instrument.

6. CONCLUSION

In this paper, we propose a new model of self-correction that is utilized to calibrate and compensate alignment errors and retardations simultaneously by measuring the SOP of target light in orbit. With a 3:1 ratio in retarder OPDs, we utilize the information of nine channels completely and discover the potential of self-correction to reduce the effects of alignment errors and environmental perturbations by target light. The target beam just needs to meet the condition of $S_1 \neq 0$ or $S_2 \neq 0$ or $S_3 \neq 0$, regardless of the SOP of the beam. The validity and feasibility of the presented method have been confirmed by simulations and experiments in the presence of alignment errors and environmental perturbations. The errors of normalized Stokes parameters by using the presented method have been reduced by 1 or 2 orders of magnitude over the traditional method. Furthermore, Monte Carlo simulations are used to confirm the accuracy of the reconstructed Stokes parameters in general conditions.

The realization of self-correction explains the ability of reducing the effects of environmental perturbations. While frequent system recalibration in the process of each measurement is necessary using the traditional method, the new method is realized only by using an effective software correction without the reference beam or any other additional components. As a result, the presented method can be used to improve the accuracy of the reconstructed Stokes parameters and the stability of the instrument effectively, which is significant for the in-orbit application of the channeled spectropolarimeter.

Funding. National Natural Science Foundation of China (NSFC) (61505199); National Research and Development Program (2016YFF0103603).

REFERENCES

1. G. van Harten, J. de Boer, J. H. H. Rietjens, A. Di Noia, F. Snik, H. Volten, J. M. Smit, O. P. Hasekamp, J. S. Henzing, and C. U. Keller, "Atmospheric aerosol characterization with a ground-based SPEX spectropolarimetric instrument," Atmos. Meas. Tech. **7**, 4341–4351 (2014).
2. N. Narukage, F. Auchere, R. Ishikawa, R. Kano, S. Tsuneta, A. R. Winebarger, and K. Kobayashi, "Vacuum ultraviolet spectropolarimeter design for precise polarization measurements," Appl. Opt. **54**, 2080–2084 (2015).
3. S. H. Jones, F. J. Iannarilli, and P. L. Kebabian, "Realization of quantitative-grade fieldable snapshot imaging spectropolarimeter," Opt. Express **12**, 6559–6573 (2004).
4. F. Yue, C. Zhang, X. Zang, D. Wen, B. D. Gerardot, S. Zhang, and X. Chen, "High-resolution grayscale image hidden in a laser beam," Light Sci. Appl. **7**, 17129 (2018).
5. M. W. Kudenov, M. E. Lowenstern, J. M. Craven, and C. F. LaCasse, "Field deployable pushbroom hyperspectral imaging polarimeter," Opt. Eng. **56**, 103107 (2017).
6. J. Craven, M. W. Kudenov, M. G. Stapelbroek, and E. L. Dereniak, "Compact infrared hyperspectral imaging polarimeter," Proc. SPIE **7695**, 769509 (2010).
7. C. Zhang, H. Wu, and J. Li, "Fourier transform hyperspectral imaging polarimeter for remote sensing," Opt. Eng. **50**, 066201 (2011).
8. S. Liu, T. Cui, Q. Xu, D. Bao, L. Du, X. Wan, W. Tang, C. Ouyang, X. Zhou, H. Yuan, H. Ma, W. Jiang, J. Han, W. Zhang, and Q. Cheng, "Anisotropic coding metamaterials and their powerful manipulation of differently polarized terahertz waves," Light Sci. Appl. **5**, e16076 (2016).
9. K. Zhanghao, L. Chen, X. Yang, M. Wang, Z. Jing, H. Han, M. Q. Zhang, D. Jin, J. Gao, and P. Xi, "Super-resolution dipole orientation mapping via polarization demodulation," Light Sci. Appl. **5**, e16166 (2016).
10. M. Dubreuil, S. Rivet, B. Le Jeune, and L. Dupont, "Time-resolved switching analysis of a ferroelectric liquid crystal by snapshot Mueller matrix polarimetry," Opt. Lett. **35**, 1019–1021 (2017).
11. M. Ren, W. Wu, W. Cai, B. Pi, X. Zhang, and J. Xu, "Reconfigurable metasurfaces that enable light polarization control by light," Light Sci. Appl. **6**, e16254 (2017).

12. H. Okabe, M. Hayakawa, H. Naito, A. Taniguchi, and K. Oka, "Spectroscopic polarimetry using channeled spectroscopic polarization state generator (CSPSG)," Opt. Express **15**, 3093–3109 (2007).
13. F. Snik, T. Karalidi, and C. U. Keller, "Spectral modulation for full linear polarimetry," Appl. Opt. **48**, 1337–1346 (2009).
14. K. Oka and T. Kato, "Spectroscopic polarimetry with a channeled spectrum," Opt. Lett. **24**, 1475–1477 (1999).
15. F. J. Iannarilli, S. H. Jones, H. E. Scott, and P. Kebabian, "Polarimetric-spectral intensity modulation (P-SIM): enabling simultaneous hyperspectral and polarimetric imaging," Proc. SPIE **3698**, 474–481 (1999).
16. J. Craven-Jones, B. M. Way, M. W. Kudenov, and J. A. Mercier, "Athermalized channeled spectropolarimetry using a biaxial potassium titanyl phosphate crystal," Opt. Lett. **38**, 1657–1659 (2013).
17. B. Wang, E. Hinds, and E. Krivoy, "Basic optical properties of the photoelastic modulator part II: residual birefringence in the optical element," Proc. SPIE **7461**, 746110 (2009).
18. T. Mu, C. Zhang, C. Jia, W. Ren, L. Zhang, and Q. Li, "Alignment and retardance errors, and compensation of a channeled spectropolarimeter," Opt. Commun. **294**, 88–95 (2013).
19. B. Yang, X. Ju, C. Yan, and J. Zhang, "Alignment errors calibration for a channeled spectropolarimeter," Opt. Express **24**, 28923–28935 (2016).
20. X. Ju, B. Yang, J. Zhang, and C. Yan, "Reduction of the effects of angle errors for a channeled spectropolarimeter," Appl. Opt. **56**, 9156–9164 (2017).
21. A. Taniguchi and K. Oka, "Stabilization of a channeled spectropolarimeter by self-calibration," Opt. Lett. **31**, 3279–3281 (2006).
22. A. M. Locke, D. S. Sabatke, E. L. Dereniak, M. R. Descour, J. P. Garcia, T. Hamilton, and R. W. McMillan, "Snapshot imaging spectropolarimeter," Proc. SPIE **4481**, 64–72 (2002).
23. D. S. Sabatke, A. M. Locke, E. L. Dereniak, and R. W. McMillan, "Linear calibration and reconstruction techniques for channeled spectropolarimetry," Opt. Express **11**, 2940–2952 (2003).
24. J. Li, J. Zhu, and H. Wu, "Compact static Fourier transform imaging spectropolarimeter based on channeled polarimeter," Opt. Lett. **35**, 3784–3786 (2010).
25. J. Craven-Jones, M. W. Kudenov, M. G. Stapelbroek, and E. L. Dereniak, "Infrared hyperspectral imaging polarimeter using birefringent prisms," Appl. Opt. **50**, 1170–1185 (2011).
26. R. Chipman, "Polarizer," in *Handbook of Optics*, M. Bass, ed. (McGraw-Hill, 1995), Chap. 13.
27. R. J. Peralta, C. Nardell, B. Cairns, E. E. Russell, L. D. Travis, M. I. Mishchenko, and R. J. Hooker, "Aerosol polarimetry sensor for the Glory Mission," Proc. SPIE **6786**, 67865L (2007).